Effects of Orbital Ordering on Electronic Communication in Multiporphyrin Arrays

Jon-Paul Strachan,[‡] Steve Gentemann,[¶] Jyoti Seth,[§] William A. Kalsbeck,[§] Jonathan S. Lindsey,*[,‡] Dewey Holten,*[,¶] and David F. Bocian*[,§]

Contribution from the Departments of Chemistry, North Carolina State University, Raleigh, North Carolina 27695-8204, Washington University, St. Louis, Missouri 63130-4899, and University of California, Riverside, California 92521-0403

Received May 22, 1997[⊗]

Abstract: The rational design of molecular photonic devices requires a thorough understanding of all factors affecting electronic communication among the various constituents. To explore how electronic factors mediate both excited- and ground-state electronic communication in multiporphyrin arrays, we have conducted a detailed static spectroscopic (absorption, fluorescence, resonance Raman, electron paramagnetic resonance), time-resolved spectroscopic (absorption, fluorescence), and electrochemical (cyclic and square-wave voltammetry, coulometry) study of tetraarylporphyrin dimers. The complexes investigated include both zinc-free base (ZnFb) and bis-Zn dimers in which the porphyrin constituents are linked via diphenylethyne groups at the *meso* positions. Comparison of dimeric arrays containing pentafluorophenyl groups at all nonlinking *meso* positions (F_{30}ZnFbU and $F_{30}Zn_2$U) with nonfluorinated analogs (ZnFbU and Zn_2U) directly probes the effects of electronic factors on intradimer communication. The major findings of the study are as follows: (1) Energy transfer from the photoexcited Zn porphyrin to the Fb porphyrin is the predominant excited-state reaction in F_{30}ZnFbU, as is also the case for ZnFbU. Energy transfer primarily proceeds via a through-bond process mediated by the diarylethyne linker. Remarkably, the energy-transfer rate is 10 times slower in F_{30}ZnFbU ($(240\ ps)^{-1}$) than in ZnFbU ($(24\ ps)^{-1}$), despite the fact that each has the same diphenylethyne linker. The attenuated energy-transfer rate in the former dimer is attributed to reduced Q-excited-state electronic coupling between the Zn and Fb porphyrins. (2) The rate of hole/electron hopping in the monooxidized bis-Zn complex, $[F_{30}Zn_2U]^+$, is ∼10-fold slower than that for $[Zn_2U]^+$. The slower hole/electron hopping rate in the former dimer reflects strongly attenuated ground-state electronic coupling. The large attenuation in excited- and ground-state electronic communication observed for the fluorine-containing dimers is attributed to a diminution in the electron-exchange matrix elements that stems from stabilization of the a_{2u} porphyrin orbital combined with changes in the electron-density distribution in this orbital. Stabilization of the porphyrin a_{2u} orbital results in a switch in the HOMO from a_{2u} in ZnFbU to a_{1u} in F_{30}ZnFbU. This orbital reversal diminishes the electron density at the peripheral positions where the linker is appended. Collectively, our studies clarify the origin of the different energy-transfer rates observed among various multiporphyrin arrays and exemplify the interconnected critical roles of a_{1u}/a_{2u} orbital ordering and linker position in the design of efficient molecular photonic devices.

I. Introduction

Understanding electronic communication is essential for the rational design and construction of functional nanoscale photonic assemblies. Electronic communication underlies both energy- and charge-transfer processes. The benchmarks for high efficiency of both of these phenomena are provided by the antenna and reaction center pigment−protein complexes of photosynthetic organisms.[1] The pigments in these proteins are tetrapyrroles that are noncovalently linked and are organized by the protein macromolecular structure. Numerous artificial photonic assemblies based on multiporphyrin architectures have been designed with the goal of achieving efficient energy and charge transfer.[2] These synthetic assemblies typically utilize a covalent linker that joins the constituents and determines the three-dimensional architecture. In these assemblies, a major issue concerns the extent of electronic communication that is mediated by the linker.

Recently, we prepared a variety of synthetic multiporphyrin arrays that include prototypical photon funnels,[3] wires,[4] and gates.[5] These arrays are all built around a semirigid[6] diarylethyne linker that mediates efficient through-bond electronic communication.[7−10] To characterize in detail the through-bond

[‡] North Carolina State University.
[¶] Washington University.
[#] University of California.
[⊗] Abstract published in *Advance ACS Abstracts*, November 1, 1997.

(1) (a) McDermott, G.; Prince, S. M.; Freer, A. A.; Hawethornthwaite-Lawless, A. M.; Papiz, M. Z.; Cogdell, R. J.; Isaacs, N. W. *Nature* **1995**, *374*, 517−521. (b) Karrasch, S.; Bullough, P. A.; Ghosh, R. *EMBO J.* **1995**, *14*, 631−638. (c) Deisenhofer, J.; Norris, J. R., Eds. *The Photosynthetic Reaction Center*; Academic: San Diego, CA 1993; Vol. II. (d) Breton, J.; Verméglio, A., Eds. *NATO Ser. A* **1992**, *237*.

(2) For reviews, see: (a) Boxer, S. G. *Biochim. Biophys. Acta* **1983**, *726*, 265−292. (b) Gust, D.; Moore, T. A. *Science* **1989**, *244*, 35−41. (c) Borovkov, V. V.; Evstigneeva, R. P.; Strekova, L. N.; Filippovich, E. I. *Russ. Chem. Rev.* **1989**, *58*, 602−619. (d) Gust, D.; Moore, T. A. *Top. Curr. Chem.* **1991**, *159*, 103−151. (e) Wasielewski, M. R. In *Chlorophylls*; Scheer, H., Ed.; CRC Press: Boca Raton, FL, 1991; pp 269−286. (f) Wasielewski, M. R. *Chem. Rev.* **1992**, *92*, 435−461. (g) Gust, D.; Moore, T. A.; Moore, A. L. *Acc. Chem. Res.* **1993**, *26*, 198−205. (h) Gribkova, S. E.; Evstigneeva, R. P.; Luzgina, V. N. *Russ. Chem. Rev.* **1993**, *62*, 963−979. (i) Kurreck, H.; Huber, M. *Angew. Chem., Int. Ed. Engl.* **1995**, *34*, 849−866.

(3) Prathapan, S.; Johnson, T. E.; Lindsey, J. S. *J. Am. Chem. Soc.* **1993**, *115*, 7519−7520.

(4) Wagner, R. W.; Lindsey, J. S. *J. Am. Chem. Soc.* **1994**, *116*, 9759−9760.

(5) Wagner, R. W.; Lindsey, J. S.; Seth, J.; Palaniappan, V.; Bocian, D. F. *J. Am. Chem. Soc.* **1996**, *118*, 3996−3997.

(6) Bothner-By, A. A.; Dadok, J.; Johnson, T. E.; Lindsey, J. S. *J. Phys. Chem.* **1996**, *100*, 17551−17557.

(7) Seth, J.; Palaniappan, V.; Johnson, T. E.; Prathapan, S.; Lindsey, J. S.; Bocian, D. F. *J. Am. Chem. Soc.* **1994**, *116*, 10578−10592.

S0002-7863(97)01678-8 CCC: $14.00

Chart 1. ZnFb Dimers with Identical Linkers but Different Energy-Transfer Rates

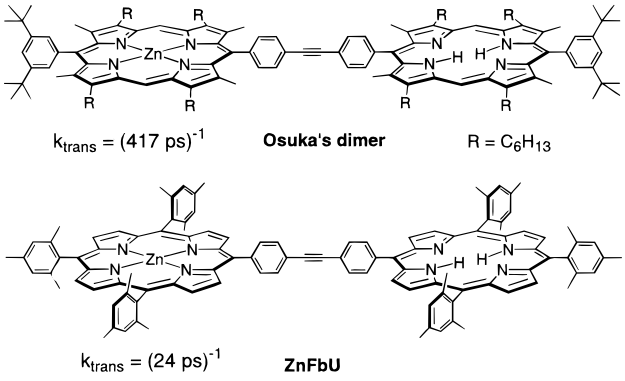

pairwise interactions that occur in the multiporphyrin arrays, we also examined a variety of diarylethyne-linked porphyrin dimers.[8−11] The effects of torsional constraints on the electronic communication were assessed by studies of singlet excited-state energy transfer[8] and ground-state hole/electron hopping[9] in dimers containing diphenylethyne or *o*-methyl-substituted diphenylethyne linkers. For the zinc-free base (ZnFb) porphyrin dimer with an unhindered diphenylethyne linker (ZnFbU), the rate of energy transfer from the photoexcited Zn porphyrin to the Fb porphyrin is ∼(24 ps)$^{-1}$, while in the ZnFb dimer having methyl groups at each of the ortho positions on the linker (ZnFbB-$(CH_3)_4$), the energy-transfer rate is slowed to ∼(115 ps)$^{-1}$.[12] The energy-transfer yields in these dimers are 99% and 95%, respectively. Hole/electron hopping studies, performed on the monocations of the bis-Zn analogs of the same diarylethyne-linked dimers, revealed that this ground-state process is ∼100-fold slower than the excited-state energy migration. Taken together, these studies constitute a first step toward understanding the role of the diarylethyne linker in mediating electronic communication.

A particularly noteworthy characteristic of our diarylethyne-linked porphyrin arrays is their rapid, highly efficient energy transfer. In contrast, a far slower (∼(417 ps)$^{-1}$) and less efficient (78%) energy transfer process was observed by Osuka et al.[13] in a dimer structurally similar to ZnFbU (Chart 1).[14] The 17-fold attenuation in the energy-transfer rate is striking considering that ZnFbU and Osuka's dimer have identical diphenylethyne linkers. Given that energy transfer is so rapid and essentially quantitative in ZnFbU,[8,10] the faster rate in this complex relative to that in Osuka's dimer cannot originate in competing pathways of depopulating the photoexcited Zn porphyrin. Instead, the faster energy-transfer rate must reflect significantly greater intradimer electronic communication. The differences in energy-transfer rates in the two dimers must ultimately derive from the nature of the porphyrins rather than the linker. In particular, ZnFbU has hydrogens at each of the eight β-pyrrole positions and has an aryl group at each of the four *meso* positions, while Osuka's dimer has alkyl groups at all β-pyrrole positions and only two *meso*-aryl substituents.

The substitution pattern at the periphery of a porphyrin can alter the ordering of the two nearly degenerate HOMOs (a_{2u}, a_{1u}).[15] The *meso*-aryl substitution pattern on ZnFbU results in a HOMO of a_{2u} symmetry, whereas the β-alkyl substitution pattern on Osuka's dimer should result in a HOMO of a_{1u} symmetry. These two porphyrinic molecular orbitals exhibit very different nodal patterns. The a_{2u} orbital has substantial electron density on the *meso*-carbon atoms, where the linker is appended. In contrast, the a_{1u} orbital has nodal planes through these atoms. We wondered whether electronic factors arising from the difference in orbital ordering could be the principal source of the different energy-transfer rates in ZnFbU versus Osuka's dimer. To test this hypothesis, we prepared a ZnFb dimer (F_{30}ZnFbU) bearing pentafluorophenyl groups at all non-linking *meso* positions while leaving the diphenylethyne linker identical with that of ZnFbU (Chart 2). Two principal reasons motivated the choice of the F_{30}ZnFbU molecular architecture. First, the strong electron-withdrawing effects of the nonlinking *meso*-pentafluorophenyl groups significantly stabilize the a_{2u} orbital with respect to the a_{1u} orbital. In metallo *meso*-tetrakis(pentafluorophenyl)porphyrins (F_{20}MTPP), this stabilization is sufficiently large that the a_{1u} orbital becomes the HOMO.[16,17] Thus, replacement of the *meso*-phenyl substituents with *meso*-pentafluorophenyl groups elicits a large change in the electronic factors for energy transfer. Second, preservation of the same diphenylethyne linker in F_{30}ZnFbU and ZnFbU should minimize any differences in linker-associated vibrational motions that modulate the energy-transfer rate. Accordingly, comparison of the excited-state energy transfer in ZnFbU versus F_{30}ZnFbU and ground-state hole/electron transfer in the cations of the corresponding bis-Zn complexes (Zn_2U and $F_{30}Zn_2$U) provides a direct probe of how electronic factors derived from a_{2u}/a_{1u} orbital ordering mediate electronic communication.

II. Results

A. Synthesis of the Porphyrin Building Blocks and Arrays. Porphyrin building blocks bearing a functional group (iodo, ethynyl) at one of the four *meso* positions provide the basis for constructing the dimeric arrays. These A_3B porphyrin building blocks can be obtained through mixed aldehyde−pyrrole condensations by using the two-step one-flask room temperature synthesis.[18] The unhindered diphenylethyne linker is ultimately derived from 4-iodobenzaldehyde (commercially available) and 4-[2-(trimethylsilyl)ethynyl]benzaldehyde.[19] The method of mixed aldehyde−pyrrole condensations affords a mixture of six porphyrins. The separability of mixtures of porphyrins by adsorption chromatography depends on the facial encumbrance due to *ortho* substituents and the different polarities of all of the aryl substituents.[20] The desired porphyrin building blocks, F_{15}FbI and F_{15}ZnU (Chart 2), were readily separated from their respective mixtures by column chromatography on silica. The Zn ethynylporphyrin F_{15}ZnU′ was prepared by deprotecting the trimethylsilyl-protected porphyrin (F_{15}ZnU) with tetrabutylammonium fluoride on silica.

(8) Hsiao, J.-S.; Krueger, B. P.; Wagner, R. W.; Delaney, J. K.; Mauzerall, D. C.; Fleming, G. R.; Lindsey, J. S.; Bocian, D. F.; Donohoe, R. J. *J. Am. Chem. Soc.* **1996**, *118*, 11181−11193.

(9) Seth, J.; Palaniappan, V.; Wagner, R. W.; Johnson, T. E.; Lindsey, J. S.; Bocian, D. F. *J. Am. Chem. Soc.* **1996**, *118*, 11194−11207.

(10) Li, F.; Gentemann, S.; Kalsbeck, W. A.; Seth, J.; Lindsey, J. S.; Holten, D.; Bocian, D. F. *J. Mater. Chem.* **1997**, *7*, 1245−1262.

(11) Wagner, R. W.; Johnson, T. E.; Lindsey, J. S. *J. Am. Chem. Soc.* **1996**, *118*, 11166−11180.

(12) The previous value for the energy-transfer rate for ZnFbB$(CH_3)_4$, k_{trans} = (88 ps)$^{-1}$, has been remeasured by transient absorption spectroscopy over a longer time frame. The revised value is k_{trans} = (115 ps)$^{-1}$, which is used throughout this paper.

(13) Osuka, A.; Tanabe, N.; Kawabata, S.; Yamazaki, I.; Nishimura, Y. *J. Org. Chem.* **1995**, *60*, 7177−7185.

(14) This energy-transfer rate has been calculated by using the formula $k_{trans} = (\tau_{Zn^*})^{-1} - (\tau^{\circ}_{Zn^*})^{-1}$ and the lifetimes reported by Osuka (τ_{Zn^*} = 326 ps, $\tau^{\circ}_{Zn^*}$ = 1.5 ns). The energy-transfer rates reported by Osuka apparently use the incorrect formula $k_{trans} = (\tau_{Zn^*})^{-1}$.

(15) Gouterman, M. In *The Porphyrins*; Dolphin, D., Ed.; Academic Press: New York, 1978; Vol. III, pp 1−165.

(16) Fujii, H. *Chem. Lett.* **1994**, 1491−1494.

(17) Spellane, J. P.; Gouterman, M.; Antipas, A.; Kim, S.; Liu, Y. C. *Inorg. Chem.* **1980**, *19*, 386−391.

(18) Lindsey, J. S.; Wagner, R. W. *J. Org. Chem.* **1989**, *54*, 828−836.

(19) Austin, W. B.; Bilow, N.; Kelleghan, W. J.; Lau, K. S. Y. *J. Org. Chem.* **1981**, *46*, 2280−2286.

(20) Lindsey, J. S.; Prathapan, S.; Johnson, T. E.; Wagner, R. W. *Tetrahedron* **1994**, *50*, 8941−8968.

Chart 2. Structures of the Dimeric Arrays and the Porphyrin Building Blocks

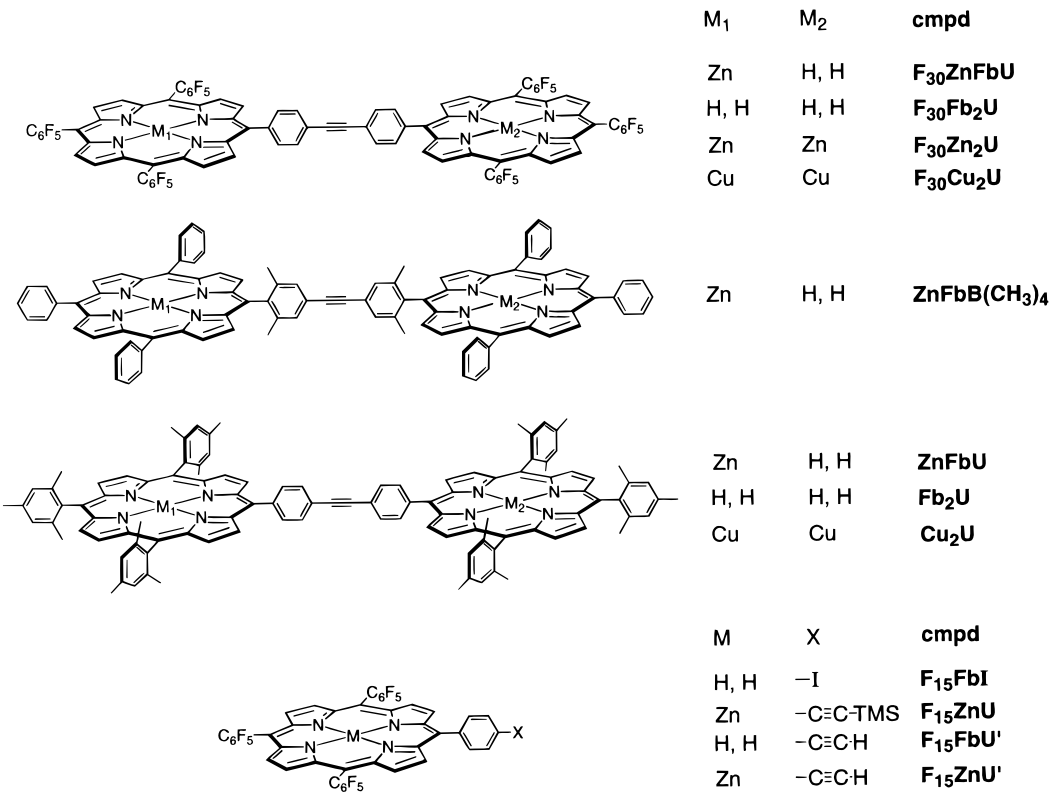

Scheme 1. Synthesis of Dimeric Arrays

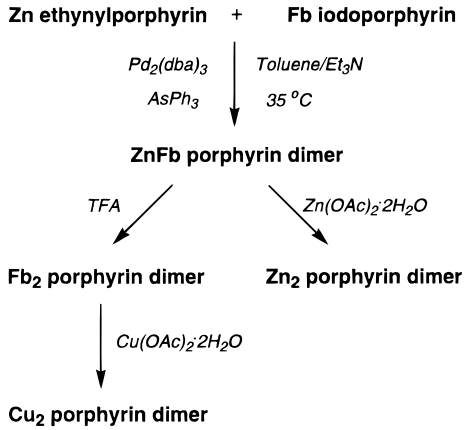

The preparation of the dimeric arrays relies on Pd-mediated coupling reactions[21] of ethynylporphyrins and iodoporphyrins (Scheme 1). The reaction of the Fb iodoporphyrin F_{15}FbI and the Zn ethynylporphyrin F_{15}ZnU′ with $Pd_2(dba)_3$ and triphenylarsine in toluene/triethylamine (5:1) at 35 °C under argon for 2 h afforded the diphenylethyne-linked dimer F_{30}ZnFbU. The crude reaction mixture consisted of small amounts of higher molecular weight material (uncharacterized), desired F_{30}ZnFbU, monomeric porphyrins, and reagents. The progress of the reaction could be assessed by silica TLC or by analytical SEC. For preparative purification, a flash silica column with hexanes−CH_2Cl_2 (1:1) removed triphenylarsine and left the Pd residue on the top of the column. Passing the resultant mixture over a preparative SEC column in THF (twice) removed the unwanted higher molecular weight material and porphyrin monomers. The fraction containing the desired F_{30}ZnFbU dimer was then passed over a silica column eluting with hexanes−CH_2Cl_2 (2:1). Fractions were assessed by analytical SEC at all stages of the purification process. This method afforded 92 mg of F_{30}ZnFbU in 81% yield, with no detectable impurities (>99%) based on integrated peak area in the analytical SEC.

The bis-Zn dimer $F_{30}Zn_2U$ was prepared in quantitative yield by treatment of the corresponding F_{30}ZnFbU dimer with methanolic zinc acetate. The bis-Cu dimers (Cu_2U, $F_{30}Cu_2U$) were prepared by treating the corresponding Fb_2 dimers (obtained by direct synthesis or by demetalating the ZnFb dimers with trifluoroacetic acid) with methanolic cupric acetate (Scheme 1). These metal insertions also were quantitative. This building block approach provided ready access to small quantities of the various dimers.

B. Physical Properties of the Neutral Complexes. (1) Absorption Spectra. The absorption spectra of selected monomeric and dimeric fluorine-containing porphyrins are shown in Figure 1. The general spectral features of all the compounds (strong B and weak Q bands) are similar to one another and similar to those we have previously reported for other arrays and their building blocks.[9,10] In particular, the absorption spectra of the dimers are approximately a superposition of the absorption spectra of the Zn and Fb porphyrin constituents, indicating the relatively weak interactions between the porphyrins. The spectra of the fluorine-containing Zn porphyrins resemble those of their nonfluorinated counterparts. In contrast, the strength of the $Q_x(0,0)$ absorption band of the fluorine-containing Fb porphyrins (e.g., F_{15}FbU′ in Figure 1) is reduced approximately 6-fold relative to that of nonfluorinated Fb porphyrins such as TPP. Integration of the $Q_x(1,0)$ and $Q_x(0,0)$ region of F_{15}FbU′ indicates that the less intense $Q_x(0,0)$ band of this complex corresponds to 40% reduction in the oscillator strength of the ground-state → Q-state transition relative to that of TPP. The same is true for the Fb component of F_{30}ZnFbU and for F_{20}TPP. The change in absorption profile alters the spectral overlap between the absorption of the Fb component and the emission of the Zn component of F_{30}ZnFbU by less than 2-fold relative to that for ZnFbU.

(2) Fluorescence Quantum Yields and Lifetimes. The fluorescence yields and lifetimes of F_{30}ZnFbU, ZnFbU, and a

(21) Wagner, R. W.; Johnson, T. E.; Li, F.; Lindsey, J. S. *J. Org. Chem.* **1995**, *60*, 5266−5273.

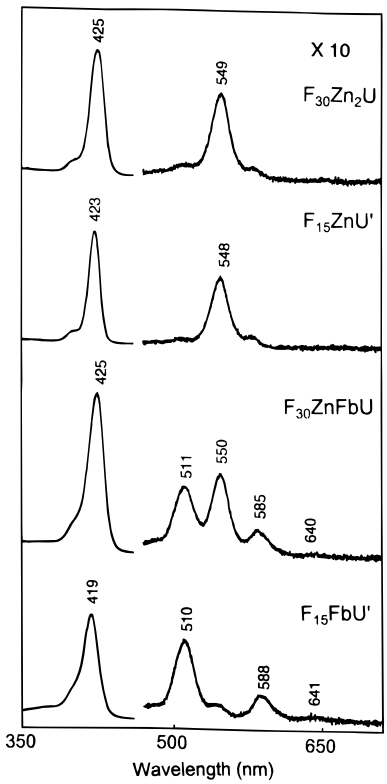

Figure 1. Absorption spectra in toluene at room temperature of the monomeric building blocks and dimeric arrays.

number of monomeric building blocks are collected in Table 1. The emission from F_{30}ZnFbU comes predominantly from the photoexcited Fb porphyrin (Fb*) independent of whether the Zn or Fb porphyrin is excited. This observation is indicative of fast and highly efficient energy transfer from the photoexcited Zn porphyrin (Zn*) to Fb, a process that is quantitated from the time-resolved absorption data (vide infra).

Although the focus of this investigation concerns energy transfer from Zn* to Fb in the ZnFb arrays, we also examined the fluorescence properties and excited state lifetimes of the fluorinated Fb porphyrins (Table 1). Unlike the Zn porphyrins, fluorination has a distinct effect on the shape of the emission spectra of the Fb porphyrin in F_{30}ZnFbU, the F_{15}FbU′ building block, and F_{20}TPP. The spectral changes mirror those observed in the absorption spectra. In particular, the ratio of the $Q_x(0,0)$ and $Q_x(0,1)$ emission bands (like the ratio of the $Q_x(0,0)$ and $Q_x(1,0)$ absorption bands) is reduced relative to the ratio in nonfluorinated complexes. Again, these spectral changes derive from an attenuated oscillator strength for ground-state ↔ Q-excited-state transitions in the fluorine-containing Fb porphyrins. Accordingly, the natural radiative rate for F_{20}TPP ($\sim$(200 ns)$^{-1}$) is reduced substantially from that for TPP[15,22] ($\sim$(120 ns)$^{-1}$). A similar effect is observed for F_{15}FbU′ and for the Fb porphyrin in F_{30}ZnFbU.

The reduced radiative (fluorescence) rate of the Fb porphyrin in F_{30}ZnFbU and its monomeric building blocks relative to the nonfluorinated analogs can account for the diminished fluorescence yields of Fb* in the fluorinated compounds (Table 1). Fluorination may also have small effects on the fluorescence yields and Fb* lifetimes via changes in the rate constants for the internal conversion and intersystem crossing decay pathways of Fb*.[23] Another potential decay pathway of Fb* that could be influenced by fluorination of the phenyl rings is charge-transfer quenching by the Zn porphyrin. However, the similarity in Fb* decay parameters for the fluorine-containing dimer and monomers in toluene indicates that, in this nonpolar solvent, there is insignificant charge-transfer quenching of Fb* by the Zn porphyrin in F_{30}ZnFbU. Charge-transfer quenching (to form Zn^+Fb^-) appears to occur to a more significant extent in the polar solvent DMSO. This process is indicated by the observation that the Fb* lifetime for F_{30}ZnFbU is reduced somewhat in DMSO relative to that in toluene (when normalized to the lifetime of the appropriate monomer building block). The effect is slightly larger in F_{30}ZnFbU than for the analogous nonfluorinated ZnFbU (Table 1).[8,10]

(3) Time-Resolved Absorption Spectra. The Zn* lifetime and the energy-transfer rate from the excited Zn porphyrin to the Fb porphyrin in F_{30}ZnFbU were monitored with ultrafast absorption difference spectroscopy. Representative data are shown in Figure 2. The 582-nm excitation flash excites both Zn and Fb porphyrins. Therefore, the absorption difference spectra acquired shortly after excitation contain features characteristic of Zn* in those arrays in which the Zn porphyrin was excited and features characteristic of Fb* in those arrays in which the Fb porphyrin was excited. The latter point is clearly seen in the absorption difference spectra acquired 1 ps after excitation of F_{30}ZnFbU (Figure 2, solid trace). The dip at 515 nm imbedded on the broad excited-state absorption arises from bleaching of the $Q_y(1,0)$ ground-state absorption band of the Fb porphyrin. The dip at 550 nm represents mostly bleaching of the Q(1,0) band of the Zn porphyrin, but it also contains a contribution of Fb porphyrin bleaching. The trough at 650 nm contains overlapping contributions of bleaching and/or stimulated emission[24] (i.e., fluorescence stimulated by the white-light pulse) from the Zn and Fb porphyrins while the dip at 715 nm is the $Q_x(0,1)$ stimulated emission characteristic of the Fb porphyrin.

The changes in the spectra that occur between 1 and 800 ps for F_{30}ZnFbU reflect the decay of Zn* and the formation, via energy transfer, of Fb* in the fraction of dimers in which the Zn porphyrin was excited. Between 1 and 800 ps, there is a decay of the Zn porphyrin bleaching at 550 nm and increases in both the Fb porphyrin bleaching at 515 nm and the Fb* stimulated emission at 715 nm. The fact that the disappearance of Zn* is accompanied by the appearance of Fb* demonstrates that energy transfer, Zn*Fb → ZnFb*, is a key pathway for decay of the photoexcited Zn porphyrin in the dimers. In fact, energy transfer is the primary mode of Zn* decay in these arrays (vide infra). The absorption difference spectrum observed following complete decay of Zn* (e.g., 800-ps spectrum) is assigned to Fb*, which is produced either by energy transfer from Zn* or via direct excitation of the Fb porphyrin (depending on which component of the dimer is excited).

(22) Seybold, P. G.; Gouterman, M. *J. Mol. Spectrosc.* **1969**, *31*, 1−13.

(23) In all of these fluorine-containing porphyrins, the reduced oscillator strength of the fluorescence transition affects the Fb* lifetime (τ) and the fluorescence yield (Φ_f) according to the relationships $\tau = (k_f + k_{ic} + k_{isc})^{-1}$ and $\Phi_f = k_f\tau$. In these expressions, k_f is the natural radiative (fluorescence) rate constant and k_{ic} and k_{isc} are the rate constants for two nonradiative decay pathways of the excited singlet state, namely internal conversion to the ground state and intersystem crossing to the excited triplet state. Assuming, as a starting point for the analysis, that the nonradiative rate constants k_{ic} and k_{isc} are not significantly affected by fluorination of the phenyl rings, the reduced natural radiative rate for F_{20}TPP relative to TPP would result in a significant ($\sim$60%) reduction in the fluorescence yield (from 0.11 to 0.07) but only a small ($\sim$5%) increase in the measured Fb* lifetime (from 13.2 ns for TPP to 13.8 ns). Indeed, the measured Φ_f of F_{20}TPP (0.049 obtained here and 0.07 previously[17]) is consistent with the view that the reduction in yield (relative to 0.11 for TPP) is due to a diminished radiative rate constant (k_f). Additionally, the measured lifetime (11.2 ns) for F_{20}TPP is only slightly shorter than that for TPP, indicating that the small increase in lifetime expected from the altered radiative rate may be counterbalanced by a correspondingly small opposing electronic or steric effect of the fluorinated phenyl rings on the nonradiative rates. Similar effects on the Fb* emission yield and lifetime are observed for F_{15}FbU′ and F_{30}ZnFbU (Table 1).

(24) Rodriguez, J.; Kirmaier, C.; Holten, D. *J. Am. Chem. Soc.* **1989**, *111*, 6500−6506.

Table 1. Singlet Excited-State Lifetimes and Fluorescence Yields[a]

		Zn porphyrin		Fb porphyrin	
porphyrin	solvent	τ (ns)	Φ_f	τ (ns)	Φ_f
dimers					
F_{30}ZnFbU	toluene	0.21	<0.002	12.9	0.057
	DMSO	0.14[b]		6.9	0.050
ZnFbU	toluene	0.026[c], 0.022[d]	<0.002[d]	13.1[c], 12.5[d]	0.13[d]
	DMSO	0.023[c]	<0.002[d]	4.3[c], 4.8[d]	0.050[d]
monomers					
F_{15}ZnU	toluene	1.7	0.025		
F_{15}ZnU′	toluene	1.6	0.022		
	DMSO	2.0	0.027		
F_{20}ZnTPP	toluene	1.4	0.019, 0.014[e]		
ZnTPP	toluene	2.2, 2.0[d]	0.033[f]		
F_{15}FbU′	toluene			13.3	0.060
	DMSO			14.0	0.089
F_{20}TPP	toluene			11.2	0.049, 0.07[e]
TPP	toluene			13.2, 11.5[d]	0.11[f]

[a] Data were collected at ~295 K. The excited-state lifetimes were determined by time-resolved fluorescence (±5%) in degassed solutions, except for lifetimes of the excited Zn porphyrins in the dimers, which were measured by using transient absorption spectroscopy (±10%). The values reported are derived from dual exponential fits to the data (see Figure 2) with the longer component fixed at the Fb* lifetime determined via fluorescence decay. [b] For F_{30}ZnFbU in DMSO, the time constant obtained in the Soret-region transient absorption (450−490 nm) is somewhat longer (160 ps) than that obtained in the region of the Q-band bleachings (500−550 nm, 115 ps). An average of the time constants determined in the two regions is reported. Further studies in other polar solvents are required to ascertain the origin of this wavelength dependence, which could derive from inhomogeneities associated with differing states of metal ligation in DMSO. [c] Reference 10. [d] Reference 8. Note that the fluorescence yields of the Zn porphyrins were scaled from those in that paper by a factor of 0.033/0.030 to account for a revised value (see footnote *f*) of the fluorescence yield of the ZnTPP standard. [e] Reference 17. [f] The yield of 0.033 for ZnTPP was used as the reference for the Zn porphyrins and the yield of 0.11 for TPP was used as the reference for the Fb porphyrins.[15,22]

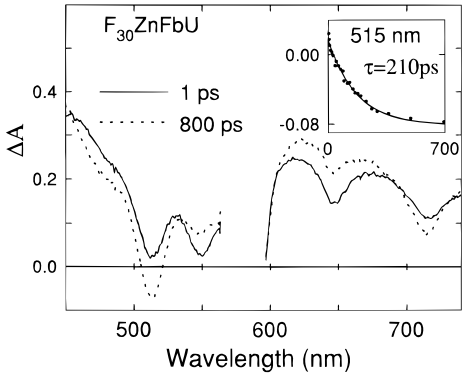

Figure 2. Transient difference spectra acquired following excitation of F_{30}ZnFbU in toluene at room temperature with a 0.2-ps flash at 582 nm. The spectra were acquired with time delays of 1 (solid traces) or 800 ps (dashed traces). Note that the data in the red region were acquired with a sample concentration ~10-fold greater than that used for the blue region. Consequently, a quantitative comparison of the absorption changes in the two regions should not be made. The inset shows a representative kinetic trace at 515 nm. The curve through the kinetic data is a fit to a dual exponential, which takes into account both the fast decay of Zn* (energy transfer) and the slow decay of Fb* (largely by intersystem crossing and internal conversion). The Fb* lifetime was fixed at the value obtained from the fluorescence lifetime measurements (Table 1). The time constant for the decay of Zn* is 210 ± 15 ps.

The inset in Figure 2 shows representative kinetic data and fits in the region of the Fb porphyrin $Q_y(1,0)$ bleaching for F_{30}ZnFbU in toluene. The fitted time constant is 210 ± 15 ps for F_{30}ZnFbU. The same time constant is obtained in other regions of the spectrum where there are sufficiently large changes in ΔA as a function of time. The time constant is assigned as the lifetime of the photoexcited Zn porphyrin. Subsequent decay of Fb* occurs with a time constant of 12.9 ns, as determined via the fluorescence decay profile (vide supra).

The intrinsic rate constant (k_{trans}) and quantum yield (Φ_{trans}) for energy transfer from photoexcited Zn porphyrin to the ground-state Fb porphyrin (Zn*Fb → ZnFb*) were obtained from the kinetic data by using the following relationships:

$$k_{trans} = (\tau_{Zn^*})^{-1} - (\tau^{\circ}_{Zn^*})^{-1} \quad (1)$$

$$\Phi_{trans} = k_{trans}\tau_{Zn^*} = 1 - \tau_{Zn^*}/\tau^{\circ}_{Zn^*} \quad (2)$$

Here, τ_{Zn^*} is the measured lifetime of the excited Zn porphyrin and $\tau^{\circ}_{Zn^*}$ is the Zn* lifetime of the relevant monomer in toluene (Table 1). This analysis assumes that the inherent rate constants for the fluorescence, internal conversion, and intersystem crossing decay pathways of Zn* have the same values in the dimer as in the corresponding monomer, and that the dramatic reduction in the Zn* lifetime in the dimer exclusively reflects energy transfer to the Fb porphyrin component. One potential process that could compete with energy transfer from Zn* to Fb is charge transfer. However, as was noted above, we see no evidence in the transient absorption data for the production of the charge-separated state Zn^+Fb^- (or Zn^-Fb^+) in toluene. We reached the same conclusion previously for the nonfluorinated dimers ZnFbU, MgFbU, and ZnFbB$(CH_3)_4$.[8,10] Along these lines, the observed Zn* lifetime is not appreciably different for F_{30}ZnFbU when the solvent is changed to DMSO, further indicating that charge transfer is not a significant decay pathway of Zn*. However, we cannot rule out a small (<10%) contribution of charge transfer to the excited-state photodynamics.

Using eqs 1 and 2 and the lifetimes in Table 1, the rates and yields of energy transfer from Zn* to Fb in F_{30}ZnFbU are calculated to be $k_{trans} = (240\ ps)^{-1}$ and $\Phi_{trans} = 87\%$. Because the calculated energy-transfer rate is nearly equal to that of the observed excited-state decay rate ($(210\ ps)^{-1}$), this analysis shows that energy transfer to the Fb porphyrin indeed dominates the decay of Zn*. Although the energy-transfer yield in F_{30}ZnFbU is high, the rate is nonetheless significantly decreased from that of ZnFbU, which exhibits $k_{trans} = (24\ ps)^{-1}$ and Φ_{trans} = 99%. We attribute the slower Zn*Fb → ZnFb* energy transfer in F_{30}ZnFbU to reduced electronic coupling.

(4) RR Spectra. The high-frequency regions of the B-state excitation (λ_{exc} = 457.9 nm) RR spectra of F_{30}ZnFbU and $F_{30}Zn_2$U are shown in Figure 3. The scattering characteristics of the porphyrin skeletal modes of the fluorine-containing arrays are similar to those observed for other arylethyne-linked arrays and are generally unremarkable.[7,9] The key spectral feature shown in the figure is the ethyne stretching mode, $\nu_{C\equiv C}$,[7,9] which

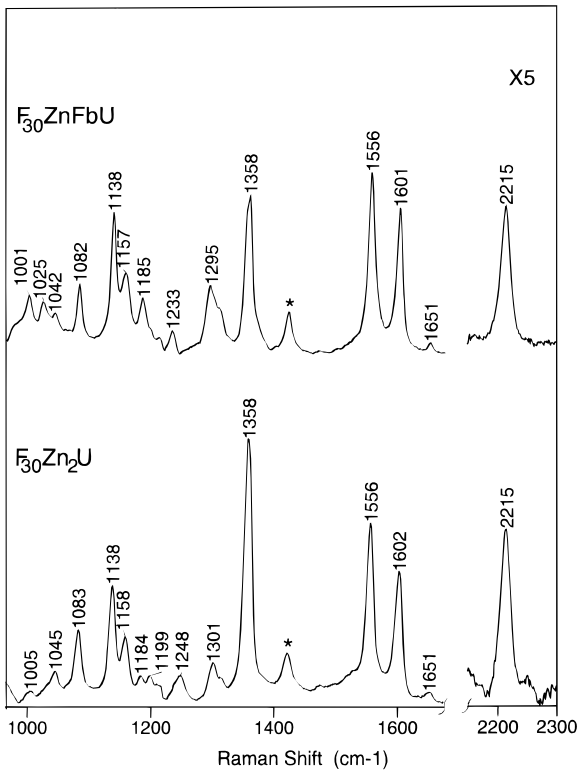

Figure 3. High-frequency regions of the B-state excitation (λ_{exc} = 457.9 nm) RR spectra of F_{30}ZnFbU and $F_{30}Zn_2U$ at room temperature. The bands marked by asterisks are due to solvent.

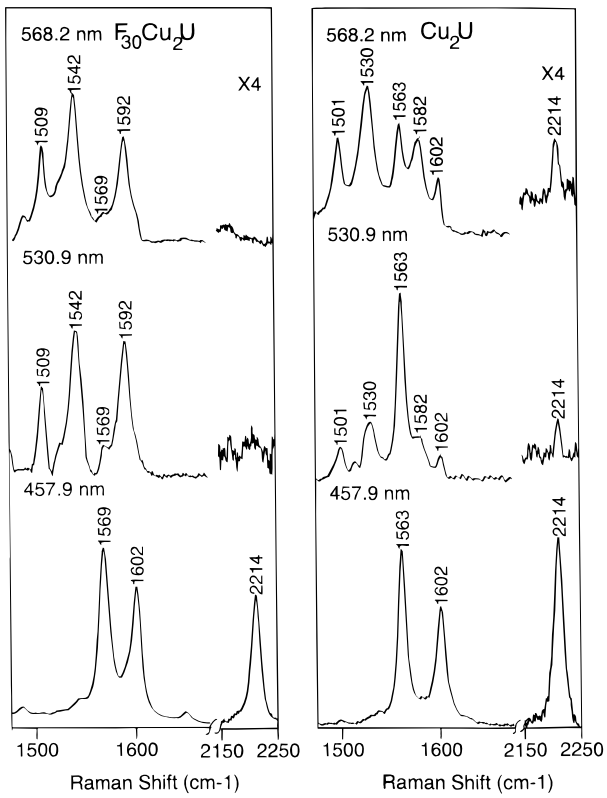

Figure 4. RR spectra of $F_{30}Cu_2U$ (left panel) and Cu_2U (right panel) obtained with B-state (λ_{exc} = 457.9 nm) and Q-state (λ_{exc} = 568.2 and 530.9 nm) excitation at room temperature.

is observed at ~2215 cm^{-1} and exhibits substantial RR intensity (relative to the porphyrin ring modes) for all the fluorine-containing dimers. The substantial RR intensity observed for the $\nu_{C\equiv C}$ modes indicates that the excited-state electronic coupling between the ethyne group and the π-system of the porphyrin ring (which dictates the relative RR intensities of the $\nu_{C\equiv C}$ versus porphyrin skeletal modes[7,9]) is appreciable for all of the arrays.

The substantial ethyne−porphyrin excited-state coupling present in the fluorine-containing arrays is, at first glance, surprising considering the relatively slow energy-transfer rate observed for F_{30}ZnFbU ($(240\ ps)^{-1}$). In this context, previous studies on ZnFbU, ZnFbB$(CH_3)_4$, and two other dimers which each contain two *o*-methyl substituents on either the Zn or Fb porphyrin unit of the linker (designated ZnFbP$(CH_3)_2$ and ZnFbD$(CH_3)_2$, respectively) have shown that the RR intensity of the $\nu_{C\equiv C}$ mode monotonically decreases as the extent of torsional constraint in the linker increases.[7,9] This decrease reflects a diminution of the excited-state electronic coupling between the ethyne group and the π-system of the porphyrin ring. Concomitantly, the energy-transfer rate monotonically decreases across the series of torsionally-constrained dimers (unhindered, ~$(24\ ps)^{-1}$ > monohindered, ~$(46\ ps)^{-1}$ > bis-hindered ~$(115\ ps)^{-1}$).[8,12] In the case of F_{30}ZnFbU, the linker is unhindered and identical with that of ZnFbU. This architectural feature is consistent with the relatively intense $\nu_{C\equiv C}$ modes in the RR spectra of both F_{30}ZnFbU and ZnFbU.[9] Yet, the energy-transfer rate is ten times slower in F_{30}ZnFbU ($(240\ ps)^{-1}$) than in ZnFbU (~$(24\ ps)^{-1}$).

The absence of apparent correlation between the RR intensity of the $\nu_{C\equiv C}$ mode and the energy-transfer rate in F_{30}ZnFbU suggests that this vibrational signature may not be a universally valid monitor of the rate. It must be noted, however, that the RR spectra shown in Figure 3 were obtained with excitation on the red edge of the B-state absorption band (λ_{exc} = 457.9 nm; λ_{Bmax} ~420 nm). In these and our previous RR studies of arylethyne-linked arrays, B-state excitation was utilized because it yields high-quality spectra and avoids interference from fluorescence inherent in Q-state-excitation RR studies of ZnFb or bis-Zn porphyrins.[7,9] Nevertheless, the energy transfer in the arrays involves the Q- rather than B-excited state. The fidelity of the B-state-excitation RR intensity of the $\nu_{C\equiv C}$ mode as an indicator of the relative energy-transfer rates in any group of arrays requires that the relative magnitude of the ethyne−porphyrin electronic coupling in the Q- versus B-excited states remains relatively constant among the members of the group and that only the absolute magnitude of the coupling (in both the Q- and B-states) varies among the members of the group. This requirement is satisfied for the torsionally constrained arrays, ZnFbU, ZnFbP$(CH_3)_2$, ZnFbD$(CH_3)_2$, and ZnFbB$(CH_3)_4$, wherein the substituents on both the linker and other aryl rings are methyl groups.[7,9] In contrast, this is clearly not satisfied for F_{30}ZnFbU.

To gain further insight into correlation between the RR intensity of the $\nu_{C\equiv C}$ mode, ethyne−porphyrin excited-state coupling, and the energy-transfer rates, RR spectra were obtained at a number of other excitation wavelengths which span both the Q- and B-state absorptions. The studies of the fluorine-containing Zn_2 and ZnFb arrays could not be extended to the Q-state region owing to interference from fluorescence; therefore, complete sets of RR spectra (B- and Q-state excitation) were instead acquired for the corresponding bis-Cu complexes, which exhibit little or no emission in the Q-state region. To make a more direct comparison with the RR spectra of $F_{30}Cu_2U$, B- and Q-state excitation RR spectra were also obtained for the Cu(II) analog of the unhindered arrays we have previously studied,[9] Cu_2U.

Figure 4 shows the high-frequency regions of the RR spectra of $F_{30}Cu_2U$ (left panel) and Cu_2U (right panel) obtained at different excitation wavelengths in the B- and Q-state regions. The absolute RR intensities observed at the different excitation wavelengths cannot be compared directly because the sample

Table 2. Half-Wave Potentials[a] for Oxidation of the Porphyrins of the Various Arrays

	Zn porphyrin		Fb porphyrin	
	$E_{1/2}(1)$	$E_{1/2}(2)$	$E_{1/2}(1)$	$E_{1/2}(2)$
$F_{15}FbU'$			1.17	1.41
$F_{15}ZnU'$	0.97	1.23		
$F_{30}ZnFbU$	0.97	1.23[b]	1.17[b]	1.41
$F_{30}Zn_2U$[c]	0.97	1.23		

[a] Obtained in CH_2Cl_2 containing 0.1 M TBAH. $E_{1/2}$ *vs* Ag/Ag^+; $E_{1/2}$ of $FeCp_2/FeCp_2^+ = 0.22$ V; scan rate = 0.1 V/s. Values are ±0.01 V. [b] Values are approximate due to overlap of Zn and Fb porphyrin waves. [c] The redox waves of the two Zn porphyrins are not resolved by cyclic voltammetry.

concentrations required to obtain reasonable quality Q-state spectra are higher than those necessary for B-state studies. The RR data do, however, provide a means of comparing the intensities of the $\nu_{C\equiv C}$ mode relative to the porphyrin modes at the different excitation wavelengths. The RR data obtained for both $F_{30}Cu_2U$ and Cu_2U show that the $\nu_{C\equiv C}$ mode exhibits appreciable RR intensity with excitation in the B-state region (λ_{exc} = 457.9 nm). This behavior parallels that observed for the fluorine-containing bis-Zn and ZnFb arrays. On the other hand, $F_{30}Cu_2U$ exhibits no discernible enhancement of the $\nu_{C\equiv C}$ mode with excitation resonant with the Q-state absorption (λ_{exc} = 568.2 or 530.9 nm). In contrast, the $\nu_{C\equiv C}$ mode of Cu_2U is clearly visible with Q-state excitation. It is not possible to quantitate the relative Q-state-excitation RR intensities of the $\nu_{C\equiv C}$ modes of $F_{30}Cu_2U$ versus Cu_2U, because this mode could not be detected for the former complex even when the sample concentration was increased substantially. The relative RR intensities of the $\nu_{C\equiv C}$ modes of $F_{30}Cu_2U$ vs Cu_2U indicate that the Q-excited-state electronic coupling between the ethyne group and the π-system of the porphyrin is much weaker for the former complex than for the latter. This observation is in accord with the significantly attenuated energy-transfer rate observed for $F_{30}ZnFbU$ versus ZnFbU (vide supra).

Hence, the data on the bis-Cu porphyrins demonstrate that the relative intensity of the $\nu_{C\equiv C}$ mode in the Q-state RR spectra is a reliable indicator of the strength of the electronic communication and correlates with the energy-transfer rate in the arylethyne-linked porphyrin arrays. On the other hand, the relative intensity of the $\nu_{C\equiv C}$ mode in the B-state RR spectra is not a good predictor of the energy-transfer efficacy in $F_{30}ZnFbU$ wherein the electronic communication between the porphyrins is substantially different in the B- versus Q-excited states. This difference in electronic communication must ultimately derive from differences in the electron density distributions in the two excited states (vide infra).

C. Physical Properties of the Oxidized Complexes. The rationale for investigating the oxidized arrays was to gain insight into the effects of changes in the relative energies of the porphyrin a_{1u} and a_{2u} orbitals on the rates of hole/electron hopping.[7,9] These rates are of interest because no independent assessment of the rates of charge transfer is available for the neutral arrays. Although the hole/electron hopping rates in the ground electronic states of the cations are not expected to be equal to the charge-transfer rates in the excited states of the neutrals, they at least provide some measure of the factors which control this type of process.

(1) Electrochemistry. The $E_{1/2}$ values for oxidation of the fluorine-containing dimeric arrays and their monomeric building blocks are summarized in Table 2. The two $E_{1/2}$ values listed in the table correspond to the first and second oxidations of the porphyrin ring.[25] The redox potentials are significantly more positive (~0.4 V) than those of the other arylethyne-substituted Zn and Fb porphyrins we have previously examined.[7,9] These latter compounds contained either unsubstituted phenyl groups or phenyl groups with mildly electron-donating substituents (methyl or methoxy). The large, positive shift in the redox potential observed for the fluorine-containing, arylethyne-substituted porphyrins parallels that observed for other heavily fluorinated porphyrins such as $F_{20}TPP$.[26,27] This shift reflects the cumulative effect of the large number of strongly electron-withdrawing fluoro substituents.[28]

Other than the shift in potentials, the redox behavior of the fluorine-containing dimeric arrays is generally similar to that we have previously reported for other arylethyne-linked arrays.[7,9] In particular, for $F_{30}ZnFbU$, four overlapping redox waves are observed, two each for the Zn and Fb porphyrins. The redox potentials of the Zn and Fb constituents of the dimer are essentially identical with those of the monomeric fluorine-containing porphyrins. For $F_{30}Zn_2U$, two redox waves are observed whose peak-to-peak separations are ~70 mV. Quantitative coulometry confirms that each wave corresponds to the removal of two electrons. Differential pulse and square-wave voltammetry on $F_{30}Zn_2U$ fails to resolve peaks due to the individual one-electron oxidations; however, the peaks exhibit asymmetries which indicate small inequivalences between the redox potentials of the individual Zn porphyrins (50 mV or less). Thus, the redox characteristics do not indicate any significant ground-state interaction between the porphyrin and arylethyne group π-systems. Indeed, such porphyrin−arylethyne group interaction is not anticipated because the $E_{1/2}$ value for oxidation of diphenylethyne is 1.64 V vs SCE[29] and its absorption λ_{max} occurs at ~300 nm,[30] indicating that the highest occupied and lowest unoccupied molecular orbitals of diphenylethyne span those of the porphyrins. Collectively, the redox characteristics of both $F_{30}ZnFbU$ and $F_{30}Zn_2U$ are indicative of relatively small ground-state electronic interaction between the porphyrin constituents.

(2) Absorption Spectra. The UV−vis absorption characteristics of the mono- and dications of the fluorine-containing arrays (not shown) are typical of those of other porphyrin π-cation radicals, namely weaker, blue-shifted B-bands and very weak, broad bands in the visible and near-infrared regions.[25a] The absorption spectra of the oxidized complexes appear to be a superposition of the spectra of the neutral and cationic species of the different porphyrin units. This observation is consistent with weak interactions between the constituent porphyrins (as also indicated by the electrochemical studies).[31−34]

(25) (a) Felton, R. H. In *The Porphyrins*; Dolphin, D., Ed.; Academic Press: New York, 1978; Vol. V, pp 53−126. (b) Davis, D. G. In *The Porphyrins*; Dolphin, D., Ed.; Academic Press: New York, 1978, Vol. V, pp 127−152.

(26) Collman, J. P.; Hampton, P. D.; Brauman, J. I. *J. Am. Chem. Soc.* **1990**, *112*, 2986−2998.

(27) (a) Barzilay, C.; Sibilia, S. A.; Spiro, T. G.; Gross, Z. *Chem.-Eur. J.* **1995**, *1*, 222−231. (b) Gross, Z.; Barzilay, C. *Angew. Chem., Int. Ed. Engl.* **1992**, *31*, 1615−1617.

(28) Ghosh, A. *J. Am. Chem. Soc.* **1995**, *117*, 4691−4699.

(29) Cariou, M.; Simonet, J. *J. Chem. Soc., Chem. Commun.* **1990**, 445−446.

(30) Armitage, J. B.; Entwistle, N.; Jones, E. R. H.; Whiting, M. C. *J. Chem. Soc.* **1954**, 147−154.

(31) Heath, G. A.; Yellowlees, L. J.; Braterman, P. S. *J. Chem. Soc., Chem. Commun.* **1981**, 287−289.

(32) Elliot, C. M.; Hershenhart, E. *J. Am. Chem. Soc.* **1982**, *104*, 7519−7526.

(33) Edwards, W. D.; Zerner, M. C. *Can. J. Chem.* **1985**, *63*, 1763−1772.

(34) (a) Angel, S. M.; DeArmond, M. K.; Donohoe, R. J.; Wertz, D. W. *J. Phys. Chem.* **1985**, *89*, 282−285. (b) Donohoe, R. J.; Tait, C. D.; DeArmond, M. K.; Wertz, D. W. *Spectrochim. Acta* **1986**, *42A*, 233−240. (c) Tait, C. D.; MacQueen, D. B.; Donohoe, R. J.; DeArmond, M. K.; Hanck, K. W.; Wertz, D. W. *J. Phys. Chem.* **1986**, *90*, 1766−1771. (d) Donohoe, R. R.; Tait, C. D.; DeArmond, M. K.; Wertz, D. W. *J. Phys. Chem.* **1986**, *90*, 3923−3926. (e) Donohoe, R. J.; Tait, C. D.; DeArmond, M. K.; Wertz, D. W. *J. Phys. Chem.* **1986**, *90*, 3927−3930.

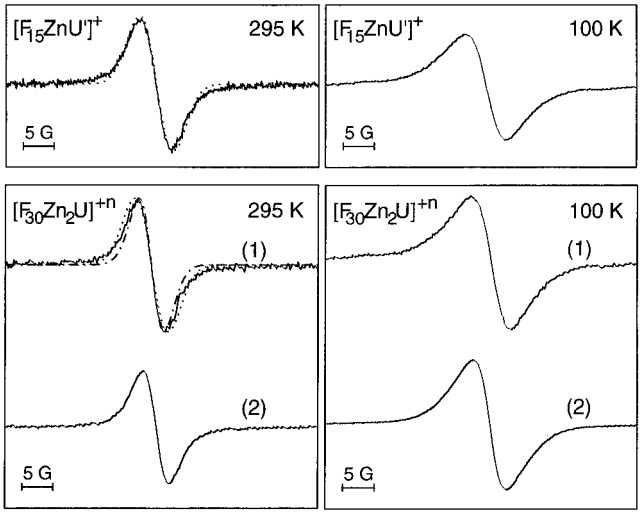

Figure 5. EPR spectra of $[F_{15}ZnU']^+$ and $[F_{30}Zn_2U]^{+n}$ obtained (n = 1, 2) at 295 and 100 K (solid lines). The additional traces shown for $[F_{15}ZnU']^+$ and $[F_{30}Zn_2U]^+$ at 295 K are simulated spectra. For $[F_{15}ZnU']^+$, the simulated spectrum was obtained with the following parameters: $a(^1H_\beta) = 1.52$ G and $a(^{14}N) = 0.36$ G; Lorentzian fwhm = 1.32 G. For $[F_{30}Zn_2U]^+$, two simulations are shown. One simulation is the same as that shown for $[F_{15}ZnU']^+$ (dotted line) and the other was obtained by reducing the hyperfine splittings by a factor of 2, doubling the number of interacting nuclei, and holding the line width constant (dot-dashed line).

(3) EPR Spectra. The EPR spectra of the oxidation products of $F_{15}ZnU'$ and $F_{30}Zn_2U$ in CH_2Cl_2 at 295 and 100 K are shown in Figure 5. The EPR spectra of all of the cations were examined as a function of sample concentration. No changes in hyperfine splittings or line shape were observed for the concentrations used for the EPR studies ($\leq$0.05 mM). Consequently, the differences observed in the spectral features of the various complexes are intrinsic and cannot be ascribed to intermolecular interactions.

The liquid solution EPR signal observed for $[F_{15}ZnU']^+$ is relatively narrow ($\sim$5.2 G) and exhibits no resolved hyperfine splittings. Similar spectral characteristics are observed in frozen solution; however, the signal is somewhat broader ($\sim$6.7 G). The general appearance of the EPR signal of $[F_{15}ZnU']^+$ is similar to that previously reported for $[F_{20}ZnTPP]^+$.[27] The ground electronic state of the latter cation is $^2A_{1u}$,[16,27] unlike most *meso*-aryl-substituted porphyrins, which typically exhibit $^2A_{2u}$ ground states.[35] The altered ground electronic state of $[F_{20}ZnTPP]^+$ is due to the significant energetic stabilization of the a_{2u} molecular orbital (which is typically the HOMO for *meso*-aryl-substituted porphyrins[15]) afforded by the presence of the strongly electron withdrawing pentafluorophenyl groups.[28] Although $F_{15}ZnU'$ contains three, rather than four, pentafluorophenyl groups, the energetic stabilization of the a_{2u} molecular orbital is sufficient to elicit a ground electronic state that is also solely, or mostly, $^2A_{1u}$ in character. This is clearly revealed by simulations of the EPR spectrum of $[F_{15}ZnU']^+$ (Figure 5, top left panel) which indicate that good quality fits can only be obtained by including substantial hyperfine splittings from the eight β-pyrrole hydrogen atoms ($a(^1H_\beta) = 1.52$ G) and very small splittings from the four pyrrole nitrogen atoms ($a(^{14}N) =$ 0.36 G). This hyperfine splitting pattern is consistent with that expected from a $^2A_{1u}$-like porphyrin π-cation radical because the a_{1u} orbital has appreciable electron density on the β-pyrrole carbon atoms and nodal planes through the pyrrole nitrogen atoms (and *meso*-carbon atoms).[15]

The liquid solution EPR spectra of $[F_{30}Zn_2U]^+$ and $[F_{30}Zn_2U]^{2+}$ are similar to one another and similar to that of $[F_{15}ZnU']^+$. In particular, both $[F_{30}Zn_2U]^+$ and $[F_{30}Zn_2U]^{2+}$ exhibit relatively narrow signals ($\sim$4.9 and 4.3 G, respectively) with no resolved hyperfine structure. The frozen solution EPR spectra of $[F_{30}Zn_2U]^+$ and $[F_{30}Zn_2U]^{2+}$ are also similar to one another and similar to that of $[F_{15}ZnU']^+$. As is the case for the latter cation, the EPR signals of both $[F_{30}Zn_2U]^+$ and $[F_{30}Zn_2U]^{2+}$ are broader in frozen solution ($\sim$6.7 and $\sim$5.5 G, respectively) than in liquid solution ($\sim$4.9 and 4.3 G, respectively). In the case of $[F_{30}Zn_2U]^{2+}$, there is no evidence for EPR signals characteristic of a triplet state in either liquid or frozen solution.[36] The latter observation indicates that the spin−spin interactions in this biradical are weak. This behavior parallels that observed for the dications of other arylethyne-linked arrays.[7,9]

The EPR characteristics observed for the $^2A_{1u}$-like $[F_{30}Zn_2U]^+$ and $[F_{30}Zn_2U]^{2+}$ cations in both liquid and frozen solution are dramatically different from those observed for the cation radicals of all the other bis-Zn arylethyne-linked dimers we have thus far investigated.[7,9] These latter arrays (which include Zn_2U and $Zn_2B(CH_3)_4$) all exhibit $^2A_{2u}$-like ground states regardless of their linker architecture. [For convenience, we will refer to this entire class of arrays as Zn_2O and designate their corresponding monomers as ZnO.] The EPR characteristics observed for the cations of ZnO and Zn_2O are as follows: (1) The liquid solution EPR line widths of both $[Zn_2O]^+$ and $[Zn_2O]^{2+}$ are much narrower than those of $[ZnO]^+$. The line narrowing observed for $[Zn_2O]^+$ is due to hole/electron hopping between the two Zn porphyrins whereas that observed for $[Zn_2O]^{2+}$ is due to exchange coupling between the two spin centers in the biradical.[7,9] The frequency of both the hole/electron hopping and exchange processes is at least an order of magnitude greater than the largest hyperfine coupling ($a(^{14}N) \sim 4.5$ MHz). (2) Upon freezing the solution, the EPR signals of $[Zn_2O]^+$ broaden and become comparable in width to those of $[ZnO]^+$ whereas the signals of $[Zn_2O]^{2+}$ exhibit additional narrowing. These spectral changes occur because the rate of hole/electron hopping is significantly attenuated and the magnitude of the exchange coupling is increased in frozen solution.[7,9]

The observation that the liquid solution EPR signals of both $[F_{30}Zn_2U]^+$ and $[F_{30}Zn_2U]^{2+}$ are comparable in width to those of $[F_{15}ZnU']^+$ suggests that frequencies of both the hole/electron hopping or exchange processes are significantly attenuated in the fluorine-containing arrays relative to those in $[Zn_2O]^+$ or $[Zn_2O]^{2+}$. The fact that the line width for $[F_{30}Zn_2U]^{2+}$ increases rather than decreases upon freezing the solution is further indicative of the attenuation of the exchange interactions. The assessment of attenuated hole/electron hopping in $[F_{30}Zn_2U]^+$ is exemplified by the results of EPR spectral simulations for this cationic array (Figure 5, bottom left panel). If the hole/electron is localized on one of the Zn porphyrins of the dimer on the EPR time scale, the number of interacting nuclei and magnitude of the hyperfine couplings should be nearly identical with that of the monomer. In contrast, if the hole/electron is delocalized, the number of interacting nuclei is twice that of the localized system whereas the hyperfine coupling constant for each of the interacting nuclei is half that of the localized system.[36] In the case of $[F_{30}Zn_2U]^+$, the observed signal cannot be adequately accounted for by using parameters commensurate with either a completely localized or delocalized hole/electron system. However, the spectra predicted using the parameters for the localized system are generally closer to the observed

(35) Fajer, J.; Davis, M. S. In *The Porphyrins*; Dolphin, D., Ed.; Academic Press: New York, 1979; Vol. IV, pp 197−256.

(36) (a) Wertz, J. E.; Bolton, J. R. *Electron Spin Resonance: Elementary Theory and Practical Applications*; McGraw-Hill: New York, 1972; pp 223−257. (b) Carrington, A.; McLachlan, A. D. *Introduction to Magnetic Resonance*; Harper and Row: New York, 1967; pp 115−131.

Table 3. Through-Bond vs Through-Space Energy-Transfer Rates and Efficiencies for Various ZnFb Dimers[a]

	ϵ_{510}[b]	ϵ_{550}[b]	Φ_f[c]	τ (ns)[c]	J (cm^6 mmol^{-1})[d]	k_{trans}^{-1} (ps)	Φ_{trans}[e]	k_{TS}^{-1} (ps)	k_{TB}^{-1} (ps)	χ_{TB}	χ_{TS}
ZnFbU	19000	7800	0.035	2.38	2.94×10^{-14}	24	0.99	745[f]	25	0.96	0.04
F_{30}ZnFbU	21000	3100	0.022	1.7	1.88×10^{-14}	240	0.87	1326	292	0.82	0.18
ZnFbB$(CH_3)_4$	22000	8900	0.032	2.26	3.53×10^{-14}	115	0.95	644[f]	140	0.82	0.18

[a] All data were obtained in toluene at room temperature [b]Peak extinction coefficients in M^{-1} cm^{-1}. [c] For the Zn porphyrin in the absence of a Fb porphyrin. [d] The Förster spectral overlap term (J) is computed using selected monomers which best approximate those units in the dimer. [e] Calculated from eq 4. [f] Previously we used an average value of $k_{TS}^{-1} = 720$ ps for the ZnFb dimers.

line shape. The results obtained for $[F_{30}Zn_2U]^+$ can be contrasted with those obtained for $[Zn_2O]^+$. The EPR line shapes observed for the latter dimeric arrays are in all cases well accounted for by using the parameters commensurate with a delocalized hole/electron system, indicating rapid hole/electron hopping on the EPR time scale.[7,9]

III. Discussion

The rational design of molecular photonic devices requires a thorough understanding of all factors that affect electronic communication among the various constituents. The studies of the fluorine-containing porphyrinic arrays reported herein have permitted exploration of how electronic factors mediate both excited- and ground-state electronic communication between the constituents in dimeric architectures. In the sections below, we first summarize the salient observations of our studies and their implications for both excited- and ground-state electronic communication. We then discuss the molecular basis for the control of electronic communication. Finally, we consider the implications of these results for the design of molecular photonic devices for efficient energy- and charge-transfer processes.

A. General Features of Electronic Communication. The first important finding of the present study is that energy transfer from the photoexcited Zn porphyrin to the Fb porphyrin is the predominant excited-state reaction in F_{30}ZnFbU. This finding is in concert with the results of our previous studies on other arylethyne-linked ZnFb dimers. However, the energy-transfer rate is 10-times slower in F_{30}ZnFbU ($(240\ ps)^{-1}$) than in ZnFbU ($(24\ ps)^{-1}$), despite the fact that each dimer contains the same diphenylethyne linker. We again emphasize that energy transfer in ZnFbU is extremely rapid and essentially quantitative. Thus, the slower dynamics observed for F_{30}ZnFbU can only be attributed to attenuated energy transfer and not to the onset of competing processes associated with fluorination of the phenyl rings. [The latter processes would only yield faster apparent energy-transfer rates than observed for ZnFbU.] The attenuated energy-transfer rate in F_{30}ZnFbU is attributed to reduced Q-excited-state electronic coupling between the Zn and Fb porphyrins in the dimer.

Although the energy-transfer rate is considerably slower in F_{30}ZnFbU than in all the other arylethyne-linked ZnFb dimers we have investigated,[8,10] the mechanism of energy transfer in this array remains predominantly through-bond (TB) rather than through-space (TS) in nature. This assessment is based on the following analysis. The observed energy-transfer rate is assumed to be due to the additive effects of through-bond (k_{TB}) and through-space (k_{TS}) processes (eq 3).[8,10] The fractional amounts of the TB (χ_{TB}) and TS (χ_{TS}) contributions can then be estimated (eqs 4 and 5). The TS energy-transfer rate can be

$$k_{trans} = k_{TB} + k_{TS} \quad (3)$$

$$\chi_{TB} = k_{TB}/k_{trans} \quad (4)$$

$$\chi_{TB} + \chi_{TS} = 1 \quad (5)$$

calculated by using the Förster theory of resonance energy transfer.[37] [Dexter (electron-exchange) mediated energy transfer also has a TS component; however, this component is negligible relative to the TS Förster contribution due to the substantial separation between the porphyrin units in the arrays.] The results of the calculations for F_{30}ZnFbU are compared with those obtained for ZnFbU and ZnFbB$(CH_3)_4$ in Table 3. The Förster calculation was performed as described previously with a point-dipole approximation.[8] The spectral overlap term (J) for these porphyrin arrays is generally in accord with those obtained for other porphyrin systems.[3,8,38] The conclusion from these calculations that the TS mechanism makes a negligible contribution to the overall energy-transfer rate is consistent with previous experimental results on torsionally-unconstrained and -constrained arrays such as ZnFbU and ZnFbB$(CH_3)_4$.[8] Furthermore, the point-dipole model provides an upper bound on the TS energy-transfer rate in F_{30}ZnFbU versus ZnFbU. This is so because the electron-withdrawing pentafluorophenyl groups redistribute electron density toward the outer periphery (away from the linker) of the two porphyrin constituents of the dimer. Thus, higher-order treatments, such as those using distributed monopoles, would predict weaker TS electronic coupling for F_{30}ZnFbU relative to that predicted by the point-dipole model.

Inspection of Table 3 reveals that the TS energy-transfer rates for all three dimers are relatively slow and differ by less than ~2-fold. F_{30}ZnFbU exhibits the slowest TS rate ($(1326\ ps)^{-1}$) owing to the low fluorescence yield of the Zn porphyrin and the diminished oscillator strength of the ground → Q-excited-state absorption transition of the Fb porphyrin. The resulting TB energy-transfer rate for F_{30}ZnFbU is $(292\ ps)^{-1}$, and this pathway accounts for ~82% of the total energy transfer. Accordingly, the TB energy-transfer rate is ~12-fold slower in F_{30}ZnFbU than in ZnFbU. It should be noted that the reduced spectral overlap, which also contributes to the TB mechanism,[37] can only account for 15−20% of the attenuation in energy-transfer rate in F_{30}ZnFbU versus ZnFbU. This is due to the fact that the spectral overlap integrals for this process, like those for the TS mechanism (Table 3), differ by less than 2-fold.[39]

The second important finding of the present study is that pentafluorophenyl groups at the nonlinking *meso* positions of

(37) Lamola, A. A. In *Energy Transfer and Organic Photochemistry*; Lamola, A. A., Turro, N. J., Eds.; Interscience: New York, 1969.

(38) (a) Anton, J. A.; Loach, P. A.; Govindjee *Photochem. Photobiol.* **1978**, *28*, 235−242. (b) Brookfield, R. L.; Ellul, H.; Harriman, A.; Porter, G. *J. Chem. Soc., Faraday Trans. 2* **1986**, *82*, 219−233. (c) Osuka, A.; Maruyama, K.; Yamazaki, I.; Tamai, N. *Chem. Phys. Lett.* **1990**, *165*, 392−396. (d) Gust, D.; Moore, T. A.; Moore, A. L.; Gao, F.; Luttrull, D.; DeGraziano, J. M.; Ma, X. C.; Makings, L. R.; Lee, S-J.; Trier, T. T.; Bittersmann, E.; Seely, G. R.; Woodward, S.; Bensasson, R. V.; Rougée, M.; De Schryver, F. C.; Van der Auweraer, M. *J. Am. Chem. Soc.* **1991**, *113*, 3638−3649. (e) Sessler, J. L.; Wang, B.; Harriman, A. *J. Am. Chem. Soc.* **1995**, *117*, 704−714.

(39) Regardless, the spectral-overlap contribution to the TB energy-transfer rate in porphyrinic systems is not a vibrational (nuclear) effect for the following reasons: (1) The oscillator strength of the Q(0,0) transition is determined almost exclusively by the energetic separation between the a_{1u} and a_{2u} orbitals and not to Franck−Condon effects. (2) The oscillator strength of the Q(1,0) transitions is derived from Herzberg−Teller coupling of the Q and B transitions and not from Franck−Condon overlaps and is essentially constant among porphyrins.[15]

the porphyrins result in significant attenuation of the ground-state electronic communication between the constituents in the dimeric arrays. The attenuated ground-state communication is manifested in the significantly slower hole/electron hopping rates observed for $[F_{30}Zn_2U]^+$ compared with the monocations of all other bis-Zn arylethyne-linked dimers studied to date.[7,9] The hole/electron hopping rates in these latter dimers have been estimated to be $\sim 10^7$ s^{-1} (or somewhat faster). In the case of $[F_{30}Zn_2U]^+$, this rate must be ~10-fold slower (comparable to or somewhat less than the largest hyperfine coupling ($a(^1H_\beta) \sim 4.35$ MHz)) to account for the characteristics of the EPR line shape.

B. Effects of Orbital Energetics and Characteristics on Electronic Communication. The extent of ground-state hole/electron hopping and excited-state energy transfer between the constituent porphyrins in the dimeric arrays is determined by the electronic and vibrational matrix elements mediated by the linker. In the case of F_{30}ZnFbU and ZnFbU (and their bis-Zn analogs), which have identical linkers (and thereby similar vibrational contributions associated with this structural element), the electronic contribution to intradimer communication is preeminent. The magnitude of the electronic contribution depends critically on the nature and electron-density distribution of the molecular orbitals that mediate the coupling between the states of the constituent porphyrins. For ZnFbU, as for most porphyrins bearing *meso*- but not β-pyrrole substituents, the HOMO has a_{2u} symmetry.[15] This molecular orbital has substantial electron density at the *meso* carbons, including those where the linker is appended. In contrast, for F_{30}ZnFbU, the pentafluorophenyl groups stabilize the a_{2u} orbital with respect to the a_{1u} orbital.[16,17] This latter molecular orbital has nodal planes at the *meso*-carbon atoms. The LUMOs of all the porphyrinic systems have e_g symmetry (D_{4h} notation). These latter orbitals also have substantial electron density at the *meso*-carbon atoms and are stabilized by the pentafluorophenyl groups. The fluorination-induced energetic stabilization of the a_{2u} orbital is sufficiently large that the a_{1u} orbital becomes the HOMO for the Zn unit, as is evidenced by the EPR signature of the monocations. Complete reversal of the a_{2u}-like and a_{1u}-like orbitals is less certain for the Fb unit;[28] however, significant energetic stabilization of the a_{2u}-like orbital is clearly apparent from the optical characteristics of this porphyrin (vide infra). An additional consequence of the extremely strong electron-withdrawing nature of the pentafluorophenyl groups is redistribution of electron density from the *meso*-carbon atoms of the a_{2u} orbital onto the pentafluorophenyl rings. No accurate information is currently available on the magnitude of this effect. Nevertheless, the optical characteristics of the pentafluorophenyl-substituted porphyrins in conjunction with the energy-transfer rates suggest that this effect is important (vide infra).

The altered energetics/characteristics of the a_{2u} versus a_{1u} molecular orbitals of the fluorine-containing porphyrins and their effect on the ground- and excited-state properties provide a reasonable explanation for the significantly attenuated electronic coupling between the constituent units in these dimeric arrays. The altered electronic coupling in the ground electronic state is more easily rationalized than that in the Q-excited states. Consequently, we will first discuss the former state and then proceed to the latter.

The orbital composition of the ground electronic state of the monocations is to a very good approximation derived from the HOMO of the porphyrin. Thus, the $^2A_{1u}$ ground state of the oxidized Zn porphyrin in $[F_{30}Zn_2U]^+$ is characterized by an absence of (or minimal) electron density at the *meso*-carbon atoms whereas the $^2A_{2u}$ ground state of the oxidized Zn porphyrin in the other arrays exhibits large density at this position. The absence of electron density at the *meso*-carbon atom, which appends the diphenylethyne linker of the fluorine-containing arrays, should naturally lead to a significant attenuation of the electron-exchange matrix element that couples the ground states of the two constituents of the dimer. The exact magnitude of the matrix element depends on the detailed composition and energetics of the ground-state wave function. At this time, high-level theoretical calculations on the dimeric arrays are not available which might address this issue.

The orbital composition of the Q-excited state of porphyrins is more complicated than that of the ground electronic state. In the four-orbital model, the Q-excited state is comprised of a configuration-interaction (CI) admixture of $a_{1u}e_g$ and $a_{2u}e_g$.[15] In both Fb and metalloporphyrins, both of these configurations contribute substantially to the Q-state. In the metallo complexes, the CI admixture is near 50/50. The optical signature of the near 50/50 admixture is the low oscillator strength of the Q(0,0) transition. (The exact value of the oscillator strength depends on the energy gap between $a_{1u}e_g$ and $a_{2u}e_g$ configurations.) The fluorination-induced stabilization of the $a_{2u}e_g$ configuration would alter the CI admixture in the Q-state(s) of both the Zn and Fb forms. This alteration would increase the contribution of the $a_{1u}e_g$ configuration to the Q-excited state(s). The changes in optical spectra of the Fb forms of the various fluorine-containing porphyrins reflect this change in configurational mixing. In this respect, the similarity of the optical spectra of the fluorine-containing and nonfluorinated Zn porphyrins is fortuitous and suggests only that the energy gap between the $a_{1u}e_g$ and $a_{2u}e_g$ configurations is similar to that in ZnTPP, but with a reversal in relative energies of the two configurations.

The diminished contribution of the $a_{2u}e_g$ configuration to the Q-excited state of the fluorine-containing porphyrins would tend to diminish the electron-exchange matrix element and, hence, the energy-transfer rate between the Zn and Fb units of the dimer. Nevertheless, the very large attenuation in energy-transfer rate in F_{30}ZnFbU is somewhat difficult to rationalize given that the $a_{2u}e_g$ configuration still makes a substantial contribution to the Q-state(s) of the porphyrins. Accordingly, additional factors must come into play in attenuating the excited-state coupling. One plausible factor is redistribution of the electron density from the *meso*-carbon atoms (including those bearing the linker) in the a_{2u} and e_g orbitals of the fluorine-containing porphyrins toward the pentafluorophenyl rings. Again, a detailed accounting of the factors that influence the electronic coupling between the Zn and Fb constituents of the dimer must await the results of accurate, high-level theoretical calculations.

The studies of the fluorine-containing porphyrins reported herein point to a logical explanation for the exceptionally slow energy-transfer rate observed in Osuka's diphenylethyne linked dimer (Chart 1). The energy-transfer rates in Osuka's dimer, F_{30}ZnFbU, and ZnFbU are $(417\ ps)^{-1}$, $(240\ ps)^{-1}$, and $(24\ ps)^{-1}$, respectively. We attribute the very slow energy-transfer rate in Osuka's dimer to a combination of predominantly electronic factors augmented by steric effects, rather than to steric factors alone.[40] In particular, the eight β-alkyl substituents and two *meso*-aryl substituents on Osuka's dimer should yield an a_{1u} HOMO, thereby diminishing the contribution of the $a_{2u}e_g$ configuration to the Q-excited state. In addition, the diphenylethyne linker is sterically constrained from rotation toward coplanarity by the methyl groups at the flanking β-pyrrole positions of the porphyrin macrocycle. Inhibited rotation toward coplanarity decreases the conjugation of the aryl unit of the linker with the porphyrin thereby diminishing electronic communication.[7,9] Indeed, the studies reported herein indicate that

(40) Kuciauskas, D.; Liddell, P. A.; Hung, S. C.; Lin, S.; Stone, S.; Seely, G. R.; Moore, A. L.; Moore, T. A.; Gust, D. *J. Phys. Chem. B* **1997**, *101*, 429−440.

the electronic coupling modulated by the nature and electron density of the HOMOs can account for at least a ~12-fold reduction in the TB energy-transfer rate [F_{30}ZnFbU (292 ps)$^{-1}$ versus ZnFbU (25 ps)$^{-1}$], whereas the electronic coupling modulated by steric factors can account for a 4−5-fold reduction [ZnFbB(CH_3)$_4$ (140 ps)$^{-1}$ versus ZnFbU (25 ps)$^{-1}$]. Together, these factors are more than sufficient to account for the ~17-fold reduction in overall energy-transfer rates in Osuka's dimer [(417 ps)$^{-1}$) versus ZnFbU ((24 ps)$^{-1}$]. Indeed, the differences in electronic coupling must be larger than the 17-fold difference in energy-transfer rates in the two types of dimers when the effects of spectral overlap are considered. In particular, the spectral overlap between Zn and Fb β-alkyl-substituted porphyrins is much larger than that for Zn and Fb *meso*-aryl-substituted porphyrins due to the much larger oscillator strength of the Q(0,0) bands of the Zn units of the β-alkyl-substituted porphyrins.[15] Thus, the increased spectral overlap alone should increase, rather than decrease, the rates of both TB and TS energy transfer in β-alkyl-substituted arrays such as Osuka's dimer relative to *meso*-aryl-substituted arrays such as ZnFbU. Accordingly, the difference in electronic communication must indeed be substantial to account for the 17-fold attenuation of the energy-transfer rate in Osuka's dimer versus ZnFbU. Again, our studies suggest that such a difference in electronic communication can be accounted for by the porphyrin a_{1u}/a_{2u} HOMO reversal plus steric constraints on the porphyrin-linker overlap. Collectively, the above assessments exemplify the critical importance of electronic structure, steric environment, and connectivity for achieving efficient electronic communication.

C. Implications for Design of Photonic Devices. The studies reported herein bear directly on the design of efficient photonic devices based on multiporphyrin architectures. In particular, our results indicate that the nature and characteristics of the molecular orbitals that participate in electronic coupling are key elements in mediating energy and charge transfer in multiporphyrin arrays. These factors have received little attention compared with other factors that are known to affect these processes (distance, orientation, energetics, and polarity of the medium).[37] Given that all cyclic polyenes have two nearly degenerate HOMOs, achieving the largest electronic coupling matrix element requires the appropriate choices of overall substitution pattern and the position of the linker. For porphyrins having a_{2u} HOMOs, covalent linkers attached at the *meso*- rather than β-pyrrole positions provide a larger magnitude of electronic coupling. Conversely, for porphyrins having a_{1u} HOMOs, covalent linkers attached at the β-pyrrole positions should afford greater electronic coupling. However, the electron density on the eight β-pyrrole positions (and the eight α-pyrrole positions) in the a_{1u} orbital is much smaller than that on the four *meso* positions (and the four central nitrogen atoms) of the a_{2u} orbital.[15] Accordingly, electronic communication mediated through the β-positions would be expected to be less efficient (for identical linkers).

Hydroporphyrins, such as chlorins and bacteriochlorins, whose natural counterparts provide efficient light-harvesting in photosynthetic organisms (chlorophylls and bacteriochlorophylls, respectively), are of great interest as potential building blocks for artificial photonic devices. Chlorins and bacteriochlorins both have a_{1u} HOMOs regardless of β-pyrrole or *meso* substitution.[15,41] Accordingly, the analysis presented here indicates that these pigments should be attached through linkers at the β-pyrrole carbons upon incorporation in molecular photonic devices to achieve the largest electronic coupling matrix element for that orbital ordering. In addition, efficient coupling requires attachment of the linker at one of the β-positions of the unsaturated rings because no appreciable density resides on the β-positions of the saturated rings. However, as noted above, the electron density at the β-position in a_{1u} orbitals is low compared with the electron density at the *meso* positions in a_{2u} orbitals. Hence, it remains to be determined whether shorter or more transmissive linkers joining chlorin β-pyrrole positions will be required to achieve the same TB energy-transfer rate as obtained in porphyrins joined via the *meso* positions. Furthermore, the greater oscillator strength of the long-wavelength transition in chlorins relative to porphyrins should commensurably enhance TS energy transfer. Model compounds must be prepared to assess the effects of positional connectivity and the resulting TS versus TB contributions to the overall energy-transfer rates and efficiencies in hydroporphyrin-based molecular photonic devices. Few covalently-linked hydroporphyrin-containing structures have been prepared for studies of intramolecular energy transfer.[2a,42] Nevertheless, it is clear from the studies presented herein that orbital ordering and the electron density distribution in the macrocycle are central determinants of the electronic communication mediated by the linker, and thereby the efficiency of the energy- and charge-transfer rates in multiporphyrin arrays. Hence, the overall combination of macrocycle type, substituent pattern, and linker position, together with orientation and other variables, must be considered in optimizing electronic coupling and the rates of energy and charge transfer in these architectures.

Acknowledgment. This work was supported by the Division of Chemical Sciences, Office of Basic Energy Sciences, Office of Energy Research, U.S. Department of Energy (J.S.L.), the LACOR Program (D.F.B.) from Los Alamos National Laboratory, and grants GM36243 (D.F.B.) and GM34685 (D.H.) from the National Institute of General Medical Sciences. Mass spectra were obtained at the Mass Spectrometry Laboratory for Biotechnology at North Carolina State University. Partial funding for the Facility was obtained from the North Carolina Biotechnology Center and the NSF.

Supporting Information Available: Complete experimental details including synthetic procedures for eight compounds and a description of physical and spectroscopic methods (10 pages). See any current masthead page for ordering and Internet access instructions.

JA971678Q

(41) Weiss, C. In *The Porphyrins*; Dolphin, D., Ed.; Academic Press: New York, 1979; Vol. III, pp 211−223.

(42) (a) Osuka, A.; Marumo, S.; Maruyama, K.; Mataga, N.; Tanaka, Y.; Taniguchi, S.; Okada, T.; Yamazaki, I.; Nishimura, Y. *Bull. Chem. Soc. Jpn.* **1995**, *68*, 262−276. (b) Osuka, A.; Marumo, S.; Wada, Y.; Yamazaki, I.; Yamazaki, T.; Shirakawa, Y.; Nishimura, Y. *Bull. Chem. Soc. Jpn.* **1995**, *68*, 2909−2915. (c) Osuka, A.; Marumo, S.; Mataga, N.; Taniguchi, S.; Okada, T.; Yamazaki, Y.; Nishimura, Y.; Ohno, T.; Nozaki, K. *J. Am. Chem. Soc.* **1996**, *118*, 155−168. (d) Osuka, A.; Wada, Y.; Maruyama, K.; Tamiaki, H. *Heterocycles* **1997**, *44*, 165−168. (e) Zheng, G.; Pandey, R. K.; Forsyth, T. P.; Kozyrev, A. N.; Dougherty, T. J.; Smith, K. M. *Tetrahedron Lett.* **1997**, *38*, 2409−2412.